Dynamical Characterization of Multi-Converter System: Simultaneous Measurement of Bus Impedance and Control Loop Gains

Tomi Roinila, *Member, IEEE*, Hessamaldin Abdollahi, Roosa Sallinen, Aram Khodamoradi, and Enrico Santi

***Abstract*—Interconnected power-electronics converters connected to a common bus have become increasingly important in various power-distribution systems. Due to interactions between converter subsystems the multi-converter system can often have stability issues even though each converter is standalone stable. Recent studies have presented a passivity-based stability criterion with which the stability of a multi-converter system can be analyzed by measuring the system bus impedance. The technique provides the stability of the complete system but does not reveal the dynamics of a single converter. The dynamics of single converters can be studied by other methods such as loop-gain measurements. The loop gains provide direct information on the operation of single converters and their stability margins but not the information about the global stability. This article combines these techniques to simultaneously analyze the single converters and the complete multi-converter system. In the method, several orthogonal perturbations are injected into the converter control loops. The current and voltage responses are measured in the loop and from the converter outputs. After this, Fourier techniques are applied to obtain the spectral information of the loop gains and the bus impedance. The applied perturbations can be designed to have a very small amplitude, and thus, the process does not cause the system to deviate too much from its normal operation. Therefore, the method is well suited, for example, in online analysis and adaptive control. Experimental measurements are presented from a complex multi-converter system. The work is a revised and extended version of a presentation at ECCE2022 (Roinila et al., 2022).**

***Index Terms*—Frequency response, signal design, spectral analysis, modeling, power system measurements.**

Manuscript received 28 February 2023; revised 8 May 2023; accepted 27 June 2023. Date of publication 4 July 2023; date of current version 22 November 2023. Paper 2023-IPCC-0094.R1, presented at the 2022 IEEE Energy Conversion Congress and Exposition (ECCE), Detroit, MI, USA, Oct. 09–13, and approved for publication in the IEEE TRANSACTIONS ON INDUSTRY APPLICATIONS by the Industrial Power Converter Committee of the IEEE Industry Applications Society [DOI: 10.1109/ECCE50734.2022.9947503]. *(Corresponding author: Tomi Roinila.)*

Tomi Roinila and Roosa Sallinen are with the Faculty of Information Technology, Communication Sciences, Tampere University, 33014 Tampere, Finland (e-mail: tomi.roinila@tuni.fi; roosa.sallinen@tuni.fi).

Hessamaldin Abdollahi and Enrico Santi are with the Department of Electrical Engineering, University of South Carolina, Columbia, SC 29208 USA (e-mail: abdollh@email.sc.edu; santi@cec.sc.edu).

Aram Khodamoradi is with the Department of Management Engineering, University of Padova, 35122 Padova, Italy (e-mail: aram.khodamoradi@phd.unipd.it).

Color versions of one or more figures in this article are available at https://doi.org/10.1109/TIA.2023.3292222.

Digital Object Identifier 10.1109/TIA.2023.3292222

I. Introduction

POWER-DISTRIBUTION systems are often dependent on the operation of multiple power-electronics converters connected to a common bus. Such interconnected converters can be found in several applications including electric vehicles [2], aircrafts [3], electric ships [4], and micro grids [5]. Such systems most often consist of a large number of power-electronics converters connected to the same bus, thus creating a complex interconnected systems.

Fig. 1 shows a conceptual diagram of a power-electronics-based distribution architecture in which the system has p buses and contains a number of interconnected switching converters. Some converters operate as a source and some converters as a load. Other converters can operate as energy-storage interface converters, and are power-bidirectional, capable of acting both as a load and source [6]. A system consisting of many converters and various sources and loads can exhibit degraded stability due to interactions between the interconnected devices even though each converter in the system is standalone stable.

Recently, nonparametric methods have become popular to analyze the stability of multi-converter systems. Such methods do not require a priori information about the system parameter or component values, and therefore, the methods are well suited for complex systems for which it would be difficult to form analytical models. A number of the previously presented methods are based either on the measurement of the equivalent bus impedances resulting from the converter interconnections [7], [8], [9], or on the loop gains of single converters [10], [11], [12]. A passivity-based stability criterion (PBSC) which directly applies to the measured bus impedance was proposed by the authors in [7] and [8]. The method was extended by a concept of an allowable impedance region (AIR) which can be used alongside the PBSC to guarantee the stability margins and dynamic performance of the system under study [9]. A different approach was applied by the authors in [13] and [12] who directly measured and analyzed the loop gains of single converters. A common advantage of all these methods is that they can be applied by nonparametric measurements of the bus-impedance or loop-gain measurements. In addition, the measurements can be applied by the existing converters in the system in real time. Therefore, the methods are well suited in online stability assessment and adaptive control.

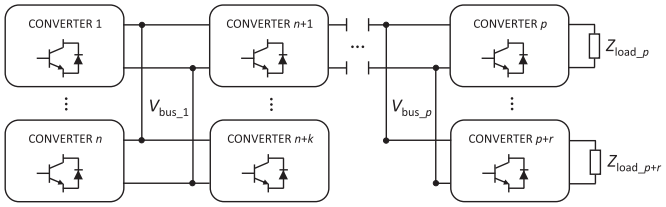

Fig. 1. Conceptual diagram of multibus system.

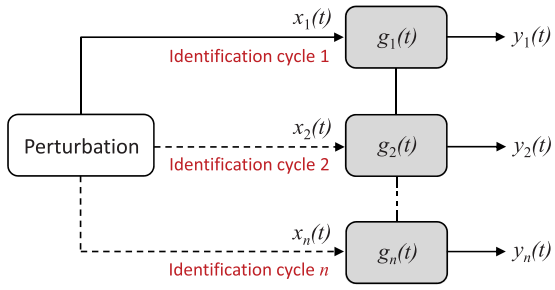

Fig. 2. Identification of MIMO system by using sequential perturbations.

Applying either the bus-impedance or loop-gain approach to analyze a multi-converter system has pros and cons. While the method based on the bus-impedance provides the dynamic performance of the complete system, the method does not reveal the effect of a single converter on the system dynamics [14]. The loop-gain approach, on the other hand, provides more direct information of the dynamics of a single converter and the stability margins but the method does not provide direct information of the overall system operation and global stability [13].

The present article combines the loop-gain and bus-impedance approaches by a method which simultaneously obtains the bus impedance and the loop gains of a multi-converter system. The method is based on orthogonal binary perturbations which are simultaneously applied by each converter in the system. Because the perturbations are orthogonal, that is, they have energy at different frequencies, the loop gains and the bus impedance can be simultaneously measured within one measurement cycle even though the converters are coupled. A specific cross-correlation technique is applied together with the orthogonal sequences to compute the frequency responses [15]. Obtaining the bus impedance and the loop gains at the same time is highly beneficial because together they produce the dynamic properties not only of the single converters but also the complete system. The method is particularly useful in a situation where some information is lost. For example, consider a case where the bus impedance is not available at given time. This may happen when communication among converters is lost. For such a scenario, the loop gain can be used as a reliable alternative because any active converter can still measure its own loop gain and adaptively improve its own stability margins.

The proposed measurement method has many advantages over the methods using sequential perturbation of the individual converters. This approach not only saves overall experimentation time, but also ensures that the bus impedance and loop gains are measured with the system in the same conditions, which may not be the case if sequential perturbations or separate experiments are applied. In addition, as the injections are binary, the sequences are very easy to implement even with a low-cost controller the output of which can only cope with a small number of signal levels. Thus, the method does not require complex external data-acquisition devices but the injections and measurements can be performed by using the existing converters in the system. It is also emphasized, that the proposed method is highly versatile, and can be applied not only for multi-converter systems but also for a wide range of other power-electronics applications.

The remainder of the article is organized as follows. Section II reviews the theory behind the cross-correlation technique and orthogonal perturbation sequences used for bus-impedance and loop-gain measurements. Section III shows simulation examples and compares the proposed method to the previously presented single-input-single-output method. Section IV demonstrates the versatility of the proposed method and presents experimental results based on a grid-connected power-distribution system. Section V discusses the issues of practical implementation of the proposed method. Finally, Section VI draws conclusions.

II. Theory and Methods

Fig. 2 shows a conceptual identification setup of a multi-converter system where each converter, represented by an impulse-response function $g_1(t), g_2(t), \ldots, g_n(t)$, is to be identified. The identification may involve input- and/or output-impedance measurements or loop-gain measurements. In a conventional identification process each converter is sequentially perturbed by an excitation signal $x_1(t), x_2(t), \ldots, x_n(t)$, producing the corresponding output response $y_1(t), y_2(t), \ldots, y_n(t)$. As the converters are most often interconnected and coupled, the superposition theorem dictates that in the identification process, when measuring the impulse-response function of one converter, no perturbation can be applied to other converters.

Assuming the multi-converter system is linear for small disturbances, the sampled output can be described as

$$y_i(m) = \sum_{k=1}^{N} g_i(k) x_i(m-k) \tag{1}$$

where N is the length of the sampled output signal, and $i = 1, 2, \ldots, N$. Assuming the excitation resembles white noise, the cross-correlation $R_{x_i y_i}(m)$ between $x_i(m)$ and $y_i(m)$ can be shown to be [16]

$$R_{x_i y_i}(m) = \alpha g_i(m) \tag{2}$$

where α denotes the variance of $x_i(m)$ and $g_i(m)$ is the system impulse response. Hence, the cross-correlation between the measured input and output signals yields the system impulse response. The response can be converted to the frequency domain and represented as a frequency-response function by applying the Fourier transform. Therefore, the frequency response is

obtained as

$$G(j\omega) = \frac{1}{\alpha}\mathcal{F}[R_{x_i y_i}(m)] \tag{3}$$

where $\mathcal{F}$ denotes the Fourier transform.

The only requirement for (3) is that the perturbation resembles white noise, that is, the autocorrelation of the perturbation must be a delta function. The method based on (3) has been applied in a number of applications of power-electronics converters and systems [17], [18], [19], [20], [21], [22]. One of the most applied perturbations has been the maximum-length binary sequence (MLBS) which is a periodic broadband sequence having only two different signal levels. The sequence has a largely controllable spectral-energy content, and, due to the binary form, the sequence is very easy to implement compared to signals of non-binary form.

A. Orthogonal Binary Perturbations

Measuring the system-characterizing frequency responses from a system depicted in Fig. 2 may become tedious as the number of required frequency responses increases. In such a case, one may apply a method based on orthogonal perturbations. In the method, several orthogonal injections are simultaneously injected into the system. As the injections are orthogonal, that is, they have energy at different frequencies, several frequency responses can be measured at the same time within one measurement cycle. The technique has several considerable advantages over the methods using sequential perturbation, This approach not only saves overall experimentation time, because the system has to be allowed to settle to a dynamic steady state only once, but also ensures that each frequency response is measured under the same system operating conditions, which may not be the case if sequential perturbations are applied.

Previous studies have widely examined the synthesis of orthogonal injection sequences applicable to MIMO systems [15]. One of the most popular approaches has been a method based on Hadamard modulation [23]. In the method, a set of orthogonal excitation sequences are obtained as follows:

1) Generate a conventional MLBS by using a shift-register circuitry with feedback.
2) The second signal is obtained by forming an inverse-repeat sequence from the MLBS; that is, by adding, modulo 2, the sequence 0 1 0 1 0 1... to the first sequence.
3) The third sequence is obtained by adding, modulo 2, the sequence 0 0 1 1 0 0 1 1... to the original MLBS.
4) The fourth sequence is obtained by adding, modulo 2, the sequence 0 0 0 0 1 1 1 1 0 0 0 0 1 1 1 1... to the original MLBS, and so on.

Fig. 3 shows samples of three orthogonal binary sequences in the time and frequency domain obtained by the presented method. The first sequence is produced by a 6-bit-length shift register. All of the sequences are generated at 10 kHz. The energy values are scaled to facilitate the illustration. The figure demonstrates the main difference between the proposed method and the conventional single-injection technique. The three signals in this example have non-zero energy only at

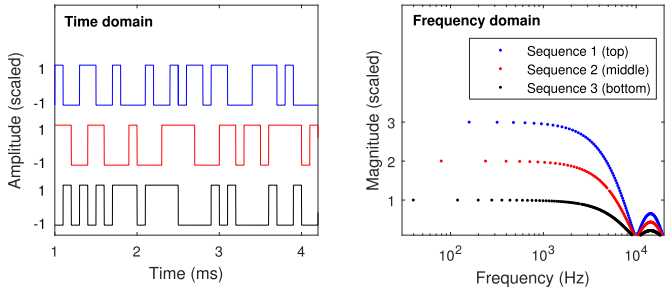

Fig. 3. Samples of three orthogonal sequences in the time and frequency domain.

different frequencies, that is, if one signal has non-zero energy at a certain frequency, the other two signals have zero energy at that frequency. Therefore, the frequency responses produced by different orthogonal sequences do not share the same frequency points making it possible to perform simultaneous measurements of different frequency responses. The orthogonal sequences have different frequency resolutions, and, thus, also the measured frequency responses will have different frequency resolutions. In practice, however, one can apply interpolation to obtain the same frequency resolution between the responses.

Fig. 3 shows that the energies of all sequences drop to zero at the generation frequency and its harmonics. The design parameters of the sequences include the signal lengths and their generation frequencies, the signal amplitudes, and the number of injection periods. These parameters can be designed based on the requirements of the frequency resolution, measurement time and SNR.

B. Injection Design

In a typical frequency-response identification, the applied perturbation should have an approximately equal amount of energy at the frequencies of interest. According to Fig. 3, the energy in the orthogonal sequences is clearly unevenly distributed over different frequencies. However, as the figure shows, the energy levels remain approximately constant at certain frequency band depending on the injection generation frequency. Therefore, approximately uniform perturbation energy can be achieved by generating the injection with a sufficiently high frequency. Typically, a value that is twice the frequency band of interest has been applied.

Other design variables of the orthogonal sequences include the period length N of the first sequence (which defines the lengths of the other sequences), number of injection periods P, and the amplitudes of the injections. The period length should be selected such that $N = 2n - 1 \geq f_{\text{gn}} \cdot T$, where n denotes the degree of the shift register used to produce the first sequence, T denotes the settling time of the system, and f_{gn} is the generation frequency of the sequences. Applying a long enough sequence length is important for avoiding time aliasing [24]. The number of excitation periods P can be decided by evaluating the power of external noise which defines the variance of the frequency-response function. Using P excitation periods the effect of noise

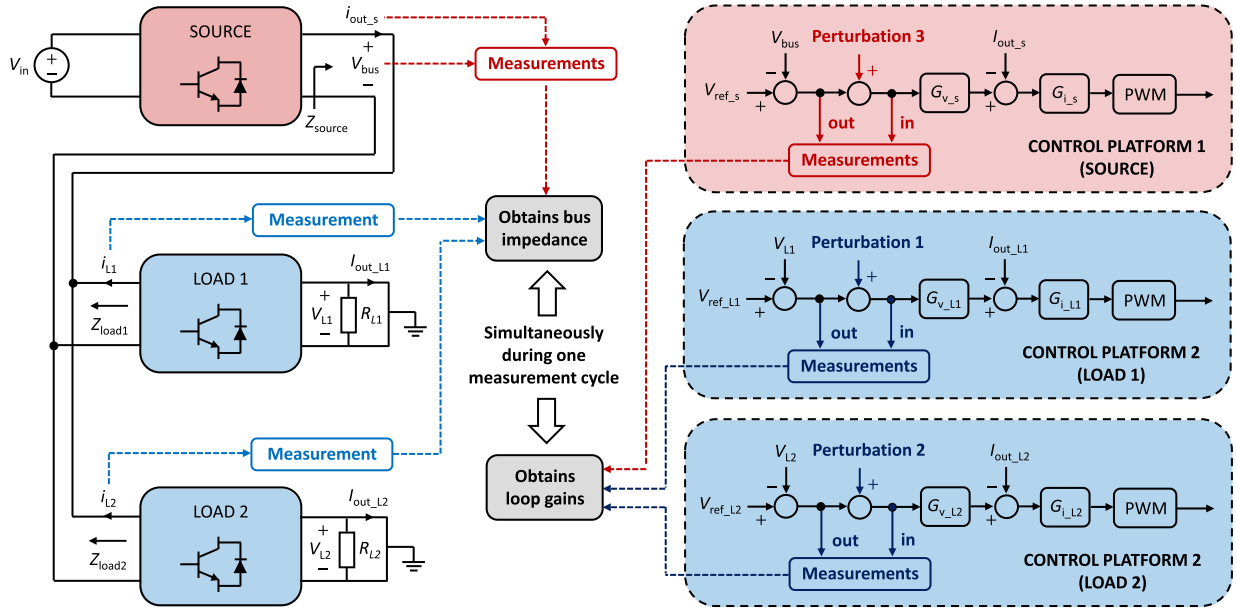

Fig. 4. Schematic diagram for measuring (simultaneously) the bus impedance and loop gains for a multi-converter system.

is reduced by $1/\sqrt{P}$. Depending on the application, different generation frequencies and number of injection periods may have to be used for each orthogonal sequence.

The amplitudes of the injections need to be chosen carefully. They have to be low enough to avoid too great effects of nonlinear dynamical phenomena but high enough to provide an adequate SNR. The nonlinearities and noise characteristics depend both on the device under test and specified operational conditions. Thus, it is difficult to give general advice for the selection of the amplitude.

Considering bus-impedance and loop-gain measurements, the starting point of the excitation design is the selection of the generation frequency f_{gn}. It is important to consider the bandwidths of the controllers as they may limit the bandwidths of the measurable frequency responses. Next, the period length N should be selected. The sequence length must be at least as high as the system settling time to avoid time aliasing.

III. Simulation Approach

Three switching converters (one source and two load converters) were connected together in Matlab/Simulink environment. Fig. 4 shows the system and the measurement setup for obtaining the bus impedance and loop gains. In the figure, $G_{\mathrm{v\_s}}$ and $G_{\mathrm{i\_s}}$ denote the voltage and current controllers of the source converter, and $G_{\mathrm{v\_L1}}$, $G_{\mathrm{i\_L1}}$, $G_{\mathrm{v\_L2}}$, and $G_{\mathrm{i\_L2}}$ are the corresponding controllers of the load converters. The main parameter values are given in Table I.

Three orthogonal binary sequences were designed. The first sequence had 1023 bits, the second 2046 bits, and the third 4092 bits. Each sequence was generated at 20 kHz. The injection amplitudes were selected such that the measured variables did not exceed their nominal values by more than 5 %. The perturbations were simultaneously injected on top of the inputs of the converter's voltage controllers. The voltages from both sides of the injection points, the output currents of each converter, and the bus voltage were simultaneously measured, and (3) was applied to each of the six input-output couple.

TABLE I
Simulation Parameters

Converter	Parameter	Value	Perturbation
Load 1	R_{L1} $V_{\mathrm{ref\_L1}}$	10 Ω 56 V	Length: 1023 bits Amplitude: 0.05 V
Load 2	R_{L2} $V_{\mathrm{ref\_L2}}$	2 Ω 41 V	Length: 2046 bits Amplitude: 0.05 V
Source	V_{in} $V_{\mathrm{ref\_s}}$	200 V 100 V	Length: 4092 bits Amplitude: 0.05 V

Fig. 5 shows the three impedances and the three loop gains measured using the proposed technique. The figure also shows the calculated bus impedance obtained by [8]

$$\frac{1}{Z_{\mathrm{bus}}(s)} = \frac{1}{2}\left\{\frac{1}{Z_{\mathrm{source}}(s)} + \frac{1}{Z_{\mathrm{load1}}(s)} + \frac{1}{Z_{\mathrm{load2}}(s)}\right\} \quad (4)$$

The references (black solid lines) were obtained by sequential measurements using the conventional MLBS (one at a time). As the figure shows, the impedances and the loop gains are accurately measured in a wide frequency band during a single measurement cycle. The left-hand-side figure shows that the phase of the bus impedance stays within ± 90 degrees in a wide frequency range. Therefore, because the impedance is passive, the system is stable. The results also show that the bus impedance closely follows the output impedance of the load converter (Load 1) except at the resonance frequency. This is expected as the output impedance of the load converter is much smaller than the impedance of the source converter and dominates in the parallel combination. The bus impedance does

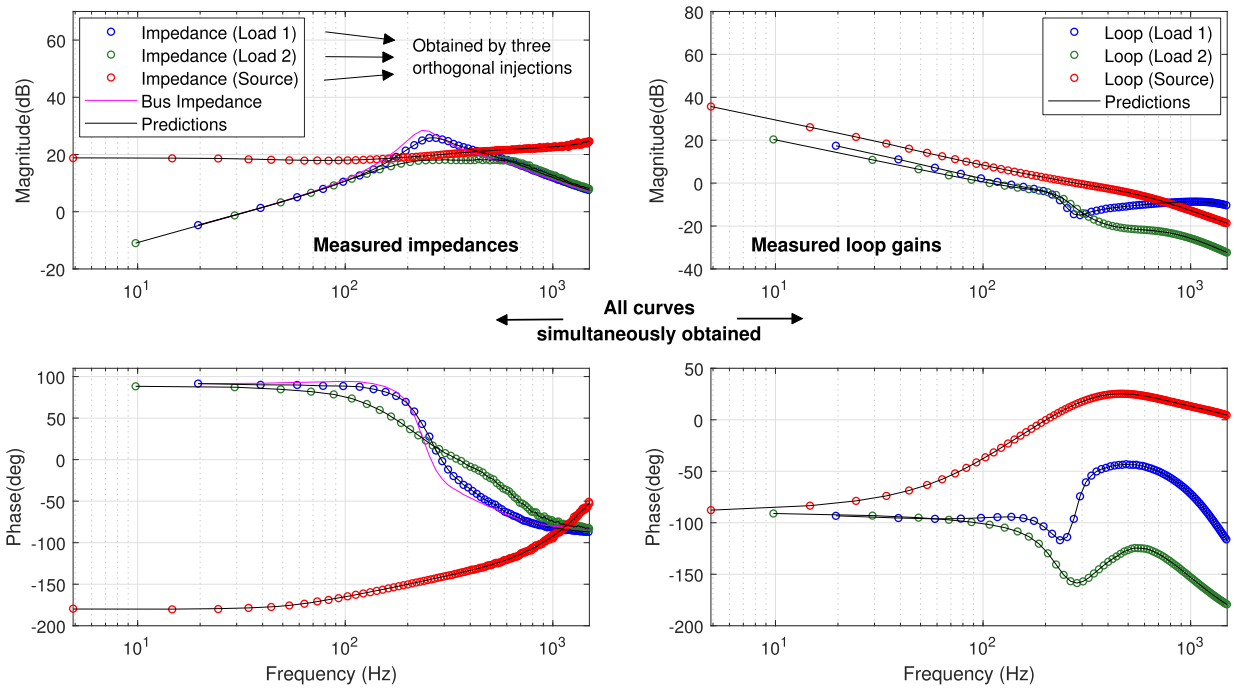

Fig. 5. Measured impedances and loop gains.

TABLE II
MEASURED FREQUENCY RESPONSES AND KEY PROPERTIES

Measured response	Perturbation	Resolution	Bandwidth
Impedance & loop (Load 1)	Sequence 1	19.6 Hz	2 kHz
Impedance & loop (Load 2)	Sequence 2	9.8 Hz	2 kHz
Impedance & loop (Source)	Sequence 3	4.9 Hz	2 kHz

not show a very high peak at the resonance indicating that the system is well damped. The loop gains shown in right-hand-side figure verify and supports the analysis of a stable system; all the controllers have more than 70 degrees of phase margin. Table II summarizes the measurement process.

It is emphasized that when performing simultaneous frequency-response measurements using orthogonal sequences it does not matter which orthogonal sequence is applied into each injection point. The only difference produced by different perturbations is seen in the frequency resolutions as the sequences do not share energy at the same frequencies. As Fig. 5 shows, each impedance curve and each loop are measured at different frequencies.

In general, the requirements for the measurement bandwidth depend on the application. In the multi-converter example used in the paper, the frequency responses are measured up to 2 kHz. This is the bandwidth in which the control design and stability analysis are performed. In the applied system, two frequency ranges are of particular interest: 1) the frequencies where the system shows a resonance and 2) the crossover frequencies of the loop gains. As Fig. 5 shows, the bus impedance exhibits a peak resonance in the mid-frequency range. The frequency and the magnitude of this resonance as well as other post-calculated characteristics of the bus impedance are usually applied for a stability assessment based on the PBSC and AIR [8]. However, in the case of multiple source converters, the bus impedance may exhibit several resonances. In such a case, other methods are required to determine the converter that produces the highest peak resonance. In order to determine the resonance, loop-gain measurements of single converters can be used. The loop gains provide the phase margins of different source converters, and the converter having the lowest margin is usually responsible for the highest peak in the bus impedance. Therefore, more efficient damping of the bus impedance (that is, higher overall system stability) is achieved by adjusting the controller gains of the converter that has the lowest phase margin.

The measurement bandwidth can be increased by increasing the generation frequency of the orthogonal sequences. As Fig. 3 shows, the sequence energy drops to zero at the generation frequency. So, increasing the generation frequency with the same sequence length will provide energy at a wider bandwidth (but there is a tradeoff as increasing the generation frequency will weaken the frequency resolution).

The greatest benefit of the orthogonal perturbations is that they can be simultaneously injected into the system (because they perturb different frequencies). This makes it possible to measure several (coupled) frequency responses at the same time. Now, if applying a conventional perturbation (for example, the traditional pseudo-random binary sequence (PRBS)) the frequency responses are sequentially obtained. That is, the perturbation is first applied to obtain the first frequency response. Then, the same perturbation is applied to obtain the second frequency response and so on. This approach not only takes more time

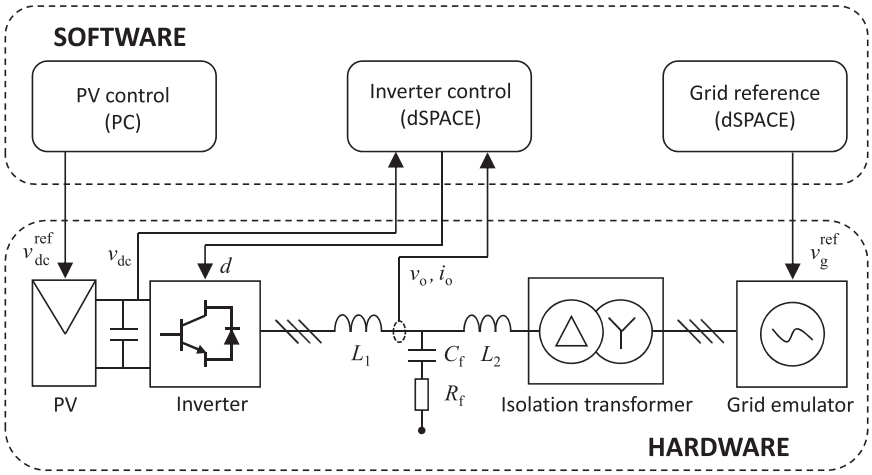

Fig. 6. System under study.

TABLE III
ELECTRICAL PARAMETERS

v_{dc}^{ref}	v_g^{ref}	f_{SW}	f_{grid}	L_1	L_2	C_f	R_f
410 V	120 V	8 kHz	60 Hz	2.5 mH	0.6 mH	10 µF	1.8 Ω

TABLE IV
PERTURBATION PARAMETERS

Target	Sequence length	Amplitude	Generation frequency	Number of periods
Inverter	2047 bits	0.2 V	4 kHz	50
Grid	4094 bits	4 V	4 kHz	100

but also poses a risk that the system operating point changes between the measurements. The measurement accuracy does not change regardless of whether the orthogonal sequences (single measurement cycle) or the conventional PRBS (multiple measurement cycles) is used. But this holds only in a simulator environment where we can guarantee that the system parameters do not change between the measurements.

IV. EXPERIMENTAL VERIFICATION

In order to demonstrate the versatility of the proposed method, several frequency responses were simultaneously measured from a grid-connected three-phase system. Fig. 6 shows the system under study. A 3 kW three-phase photovoltaic inverter is connected to a grid emulator through an LCL-filter and isolation transformer. The grid impedance is composed of a series-connected three-phase inductance (4.0 mH). The inverter is fed by an electric photovoltaic emulator (Spitzenberg PVS 7000), and the grid is emulated using a three-phase linear amplifier, which can sink all of the generated power (Spitzenberg PAS 5000). The inverter utilizes a conventional dq-domain current control and a cascaded dc-voltage control. The electrical parameters are shown in Table III.

Two orthogonal binary sequences were designed in order to simultaneously measure the inverter's voltage-controller loop gain, the inverter output admittance, and the grid impedance. The first sequence had 2047 bits and the second 4094 bits. Each sequence was generated at 4 kHz. The injection amplitudes were selected so that the measured voltages and currents did not exceed their nominal values by more than 10%. The first sequence was injected on top of the inverter's voltage-controller reference with 100 periods and the second sequence on top of the reference voltage (q-component) of the grid emulator with 50 periods (because the length of the second sequence is twice compared to the first sequence). Therefore, the total injection time was approximately 51 s. Fig. 7 shows a conceptual diagram of the measurement setup. The main parameter values of the applied orthogonal sequences are given in Table IV.

The data acquisition and post processing were performed as follows.

- *Loop gain:* the voltages from both sides of the injection point were measured after which (3) was applied. The measurements were averaged over 100 injection periods.
- *Inverter output admittance:* the inverter output voltages and currents were measured and transformed into the dq domain after which (3) was applied. The measurements were averaged over 50 injection periods.
- *Grid impedance:* the output voltages and currents of the grid emulator were measured and transformed into the dq domain after which (3) was applied. The measurements were averaged over 100 injection periods.

Fig. 8 shows a sample of the measured output voltages and currents before and after the injections. Fig. 9 shows the measured grid impedance, voltage-controller loop gain, and inverter output admittance. The grid impedance and the loop gain were obtained by Perturbation 1, and the inverter output admittance by Perturbation 2. In this example, only the q-components are shown for the grid impedance and for the inverter output admittance. The d-components were measured as well and they showed similar behavior. As the figure shows, the frequency

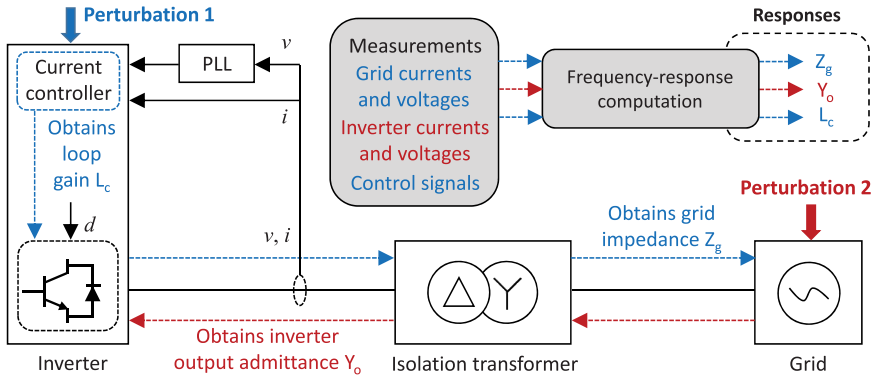

Fig. 7. Conceptual diagram of the measurement setup.

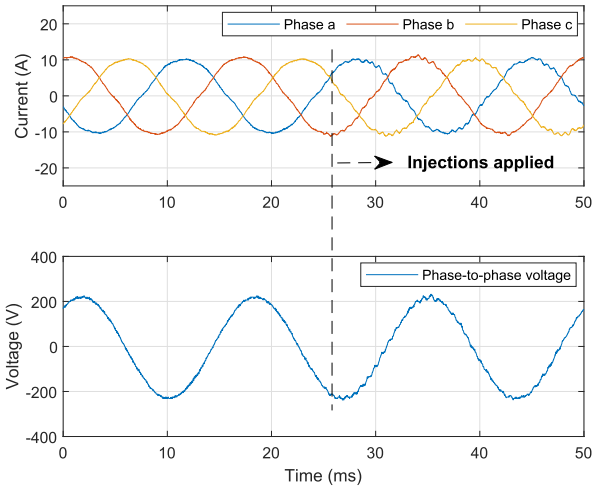

Fig. 8. Sample of grid current and voltage responses before and during the injections.

TABLE V
MEASURED FREQUENCY RESPONSES AND KEY PROPERTIES

Measured response	Perturbation	Resolution	Bandwidth
Grid impedance	Sequence 1	1.95 Hz	2 kHz
Loop gain	Sequence 1	1.95 Hz	2 kHz
Inverter output admittance	Sequence 2	0.98 Hz	2 kHz

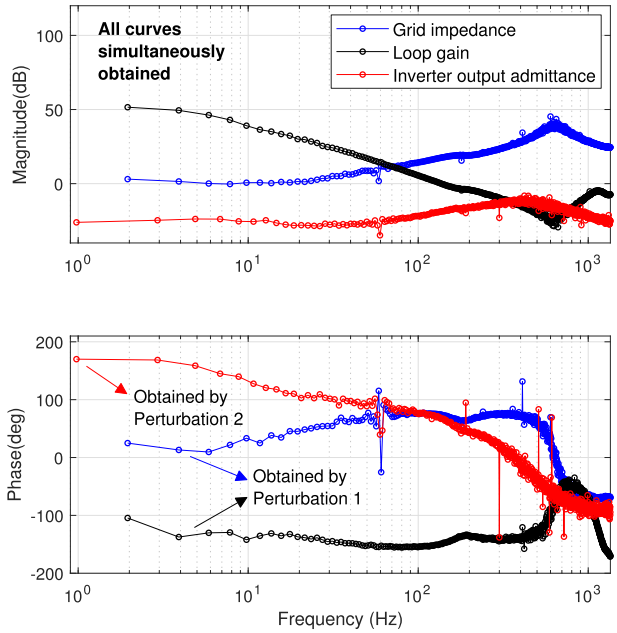

Fig. 9. Measured q-components of grid impedance, voltage-controller loop gain, and inverter output admittance.

responses are consistently obtained in a wide frequency range with a relatively low variance. The orthogonality of the perturbations can be observed as the inverter output admittance is obtained at different frequencies compared to the other two responses. The frequency responses shown in Fig. 9 confirm a stable operation of the system. The values of the grid impedance and the inverter output admittance indicate that the system has a 120-degree phase margin based on impedance-based stability criterion for grid-connected converters [25]. The measured loop gain indicates that the current controller has a phase margin of approximately 35 degrees. Table V summarizes the measurement process.

V. DISCUSSION: PRACTICAL IMPLEMENTATION

Considering a fully automated bus-impedance and loop-gain measurement by using the proposed method one of the major challenges is to find a suitable excitation amplitude for each orthogonal sequence. The amplitude has to be low enough to avoid too strong nonlinear distortions but high enough compared to noise for obtaining good enough signal-to-noise ratio. This problem is not well studied in the practical system identification of converter systems. There are, however, several methods to approach this problem such as the use of a pre-excitation signal, for example, a ramp signal [26], and iterate the range for an appropriate injection amplitude. Another technique to define the injection amplitude would be using a specific data-analysis tool

such as an uncertainty analysis [16]. These techniques add some complexity to the proposed method but certainly not too much considering modern microcircuit technology.

Another challenge in practical implementation of the proposed method is to define the requirements for the analog-to-digital-conversion quantization interval. The quantization problem was studied during the work by simulator-based analog-to-digital converter. The quantization interval was increased around the expected signal levels and only a small error was observed in the measured frequency responses. The observation can be explained by the fact that the ripple at switching frequency behaves as a dither that randomizes the quantization error thus minimizing the quantization effect [27].

VI. Conclusion

Bus impedance and loop gains are important quantities for stability analysis and control design of interconnected systems that consist of multiple power converters. This article has presented a method based on cross-correlation technique and orthogonal binary sequences to simultaneously measure the bus impedance and loop gains of interconnected multi-converter system. Applying the proposed method, the bus impedance and the loop gains can be measured within a single measurement cycle, therefore guaranteeing constant operating conditions during the experiments. Due to the binary form of the perturbations, the method is well implementable even by using a low-cost signal generator. Experimental measurements based on a grid-connected converter were presented to demonstrate the effectiveness and versatility of the proposed method.

References

[1] T. Roinila, H. Abdollahi, R. Sallinen, A. Khodamoradi, and E. Santi, "Simultaneous measurement of bus impedance and control loop gains in multi-converter systems," in *Proc. IEEE Energy Convers. Congr. Expo.*, 2022, pp. 1–6.

[2] C. Yuan, H. Bai, R. Ma, and Y. Huangfu, "Large-signal stability analysis and design of finite-time controller for the electric vehicle DC power system," *IEEE Trans. Ind. Appl.*, vol. 58, no. 1, pp. 868–878, Jan./Feb. 2022.

[3] Y. Jia and K. Rajashekara, "An induction generator-based AC/DC hybrid electric power generation system for more electric aircraft," *IEEE Trans. Ind. Appl.*, vol. 53, no. 3, pp. 2485–2494, May/Jun. 2017.

[4] G. Sulligoi, A. Vicenzutti, and R. Menis, "All-electric ship design: From electrical propulsion to integrated electrical and electronic power systems," *IEEE Trans. Transp. Electrific.*, vol. 2, no. 4, pp. 507–521, Dec. 2016.

[5] S. Lu, L. Wang, T.-M. Lo, and A. Prokhorov, "Integration of wind power and wave power generation systems using a DC microgrid," *IEEE Trans. Ind. Appl.*, vol. 51, no. 4, pp. 2753–2761, Jul./Aug. 2015.

[6] R.-M. Sallinen and T. Roinila, "Adaptive bus-impedance-damping control of multi-converter system applying bidirectional converters," *IEEE Trans. Emerg. Sel. Topics Power Electron.*, vol. 11, no. 1, pp. 567–575, Feb. 2023.

[7] A. Riccobono and E. Santi, "Comprehensive review of stability criteria for DC power distribution systems," *IEEE Trans. Ind. Appl.*, vol. 50, no. 5, pp. 3525–3535, Sep./Oct. 2014.

[8] J. Siegers, S. Arrua, and E. Santi, "Stabilizing controller design for multi-bus MVdc distribution systems using a passivity-based stability criterion and positive feedforward control," *IEEE Trans. Emerg. Sel. Topics Power Electron.*, vol. 5, no. 1, pp. 14–27, Mar. 2017.

[9] J. Siegers, S. Arrua, and E. Santi, "Allowable bus impedance region for MVDC distribution systems and stabilizing controller design using positive feed-forward control," in *Proc. IEEE Energy Convers. Congr. Expo.*, 2016, pp. 1–8.

[10] J. Lin, M. Su, Y. Sun, S. Xie, W. Xiong, and X. Li, "Unified SISO loop gain modeling, measurement, and stability analysis of three-phase voltage source converters," *IEEE Trans. Energy Convers.*, vol. 37, no. 3, pp. 1907–1920, Sep. 2022.

[11] X. Ruan et al., "Reconsideration of loop gain and its measurement in DC-DC converters," *IEEE Trans. Power Electron.*, vol. 34, no. 7, pp. 6906–6921, Jul. 2019.

[12] A. Khodamoradi, G. Liu, P. Mattavelli, and T. Messo, "Simultaneous identification of multiple control loops in DC microgrid power converters," *IEEE Trans. Ind. Electron.*, vol. 67, no. 12, pp. 10641–10651, Dec. 2020.

[13] A. Khodamoradi, G. Liu, P. Mattavelli, T. Caldognetto, and P. Magnone, "Analysis of an online stability monitoring approach for DC microgrid power converters," *IEEE Trans. Power Electron.*, vol. 34, no. 5, pp. 4794–4806, May 2019.

[14] T. Roinila, H. Abdollahi, S. Arrua, and E. Santi, "Real-time stability analysis and control of multi-converter systems by using MIMO-identification techniques," *IEEE Trans. Power Electron.*, vol. 34, no. 4, pp. 3948–3957, Apr. 2019.

[15] A. Tan and K. Godfrey, *Industrial Process Identification - Perturbation Signal Design and Applications*. Berlin, Germany: Springer, 2019.

[16] T. Roinila, T. Helin, M. Vilkko, T. Suntio, and H. Koivisto, "Circular correlation based identification of switching power converter with uncertainty analysis using fuzzy density approach," *Simul. Modelling Pract. Theory*, vol. 17, pp. 1043–1058, 2009.

[17] L. Shelembe and P. Barendse, "An adaptive amplitude-modulated pseudo-random binary sequence excitation for converter-based impedance spectroscopy characterization of photovoltaic modules," *IEEE Trans. Ind. Appl.*, vol. 59, no. 2, pp. 2007–2018, Mar./Apr. 2023.

[18] B. Miao, R. Zane, and D. Maksimovic, "System identification of power converters with digital control through cross-correlation methods," *IEEE Trans. Power Electron.*, vol. 20, no. 5, pp. 1093–1099, Sep. 2005.

[19] H. Abdollahi, S. Arrua, T. Roinila, and E. Santi, "A novel dc power distribution system stabilization method based on adaptive resonance-enhanced voltage controller," *IEEE Trans. Ind. Electron.*, vol. 66, no. 7, pp. 5653–5662, Jul. 2019.

[20] T. Roinila, H. Abdollahi, and E. Santi, "Frequency-domain identification based on pseudorandom sequences in analysis and control of DC power distribution systems: A review," *IEEE Trans. Power Electron.*, vol. 36, no. 4, pp. 3744–3756, Apr. 2021.

[21] A. Riccobono et al., "Stability of shipboard dc power distribution: Online impedance-based systems methods," *IEEE Electrific. Mag.*, vol. 5, no. 3, pp. 55–67, Sep. 2017.

[22] R. Keskin, I. Aliskan, and E. Das, "Multi-variable modeling and system identification of an interleaved boost converter," in *Proc. 13th Int. Conf. Elect. Electron. Eng.*, 2021, pp. 550–554.

[23] K. Godfrey, *Perturbation Signals for System Identification*. London, U.K.: Prentice Hall, 1993.

[24] R. Pintelon and J. Schoukens, *System Identification - A Frequency Domain Approach.* Hoboken, NJ, USA: Wiley, 2001.

[25] J. Sun, "Impedance-based stability criterion for grid-connected inverters," *IEEE Trans. Power Electron.*, vol. 26, no. 11, pp. 3075–3078, Nov. 2011.

[26] R. Dorf and R. Bishop, *Modern Control Systems*. Englewood Cliffs, NJ, USA: Prentice-Hall Inc., 2001.

[27] L. Schuchman, "Dither signals and their effect on quantization noise," *IEEE Trans. Commun. Technol.*, vol. 12, no. 4, pp. 162–165, Dec. 1964.